

## Temperature effects on counterion binding to spherical polyelectrolytes: the charge–discharge transition of lignosulfonate

Salvador Mafé <sup>a,\*</sup>, José A. Manzanares <sup>a</sup>, Anna-Kaisa Kontturi <sup>b</sup>, Kyösti Kontturi <sup>b</sup>

<sup>a</sup> *Departamento de Termodinámica, Facultad de Física, Universidad de Valencia, E-46100 Burjassot, Spain*

<sup>b</sup> *Laboratory of Physical Chemistry and Electrochemistry, Helsinki University of Technology, SF-02150 Espoo, Finland*

Received 24 October 1994

### Abstract

The effect of temperature on the effective charge numbers and diffusion coefficients of polyelectrolytes has not been dealt with in many studies. The present study concerns the temperature behavior of lignosulfonate. Lignosulfonate is a polydisperse polyelectrolyte whose molecules are compact spheres in aqueous solutions. One of its most remarkable properties is that it loses its charge in 0.1 M NaCl aqueous solution at about 40°C. In order to explain this charge–discharge transition, a theory for ion binding to spherical polyelectrolytes based on the relative population of two hydration states of the charged groups is presented. The water molecules adjacent to the charged groups are assumed to be arranged in two hydration shells, a tightly bound inner shell and an outer shell which is necessary for the group to keep its charge. The theory incorporates the ideas of the so-called “*n*-states” models employed in the study of biopolymers and membrane ionomers. The classical approaches describing ion association in electrolyte solutions consider the solvent as a dielectric continuum, and cannot explain the sharp transition of the charge number with temperature. Since many macromolecules of biological importance (e.g. globular proteins) behave as spherical polyelectrolytes, and since their effective charge numbers determine their physicochemical properties in solution, the theory considered here could also be of utility for describing temperature effects on counterion binding in spherical macromolecules other than lignosulfonate.

**Keywords:** Spherical polyelectrolytes; Lignosulfonate; Counterion binding; Charge transition

### 1. Introduction

Knowledge of the diffusion coefficients and effective charge numbers of polyelectrolytes in solution is essential, for example for the design of separation processes, for the understanding of ion-binding phenomena, and for the description of polyelectrolyte adsorption to interfaces. The polyelectrolyte radius can be obtained from the measured diffusion coefficient and the Stokes–Einstein equation. Also, evaluation of the zeta-potential from the surface charge density is possible after measuring the charge number and the polyelectrolyte radius.

The effect of temperature on the effective charge numbers and diffusion coefficients of polyelectrolytes has not been dealt with in many studies. Most measurements have been conducted at room temperature, in spite of the fact that many important polyelectrolytes such as proteins operate at higher temperatures (i.e. at  $\approx 40^\circ\text{C}$ ). Lignosulfonate

is a polydisperse polyelectrolyte whose molecules are compact spheres in aqueous solutions [1], though the application of external electric fields can transform these compact spheres into non-free unwinding coils [2]. A recent study [1] showed that lignosulfonate in 0.1 M NaCl aqueous solution lost its charge at about 40°C. The observed “charge–discharge” transition was reported to occur over a relatively small temperature range. A similar behavior was observed with cytochrome *c* (a globular protein) in 0.1 M NaCl aqueous solution [3]. The effective charge number of cytochrome *c* decreased slightly in the temperature range 10–30°C, but became suddenly zero at ca. 40°C. It must be stressed that cytochrome *c* is an interesting model compound because it is stable, its structure is well known, and it has an important biological function.

The resemblance between the two charged macromolecules mentioned above is not very remarkable except for their similar conformational structure. Since other linear polyelectrolytes (such as polystyrene sulfonate) having an unwinding coil conformation do not lose their charge at

\* Corresponding author.

this temperature [4], the charge–discharge transition might have something to do with the spherical conformation. This observation led to extensive experimental studies of the effect of temperature on the effective charge number of lignosulfonate [1–4]. Lignosulfonate was chosen as a model substance because of its polydisperse nature, and information on the conformational structure was obtained from the exponent  $b$  in the Mark–Houwink equation  $D = KM^{-b}$ , where  $D$  is the diffusion coefficient,  $K$  a constant characteristic of the macromolecule, and  $M$  the molar mass of the macromolecule [1,2]. For a compact (Einstein) sphere  $b = 1/3$ , while  $b = 1/2$  for a non-free unwinding coil.

To elucidate the loss of charge of the spherical polyelectrolyte at elevated temperatures, the effects of the following system parameters were studied: counterion nature (charge number, hydration properties, etc.) [1,4], concentration of supporting electrolyte (sodium chloride) [4], solvent dielectric constant [5], pH [6], and external electric field strength [2]. Effective charge numbers and diffusion coefficients were measured in a convective diffusion process through a porous membrane, as described in detail elsewhere [1,6]. The effective charge number is smaller than the stoichiometric charge number because of the counterion association phenomenon [1].

Despite the thorough experimental studies carried out during recent years [1–6], a quantitative theory capable of describing the charge–discharge transition of lignosulfonate and suggesting new relevant experiments is still lacking. We have addressed this question here, convinced that giving a general theory could also be of utility in the study of ion association in other spherical charged macromolecules. We propose a simple physical model based on the relative population of two hydration states of the polyelectrolyte which aims to explain the following experimental observations (see Refs. [1–5] as well as the new additional experimental results reported in this paper.

(i) *The effect of temperature ( $t$ ):*

The polyelectrolyte charge number (absolute value)  $z_p$  decreases slightly with temperature in the range 10–30°C (except for the lowest molar mass fraction,  $M = 5000$ ) but suddenly becomes zero at some transition temperature  $t_i$  in the range 35–50°C, the temperature transition region being of some 4–8°C. The classical theories for ion association (e.g., Bjerrum and Fuoss theories [7]) cannot explain this sharp charge–discharge transition.

(ii) *The effect of supporting electrolyte concentration ( $c$ ):*

The higher the sodium chloride concentration, the lower the transition temperature ( $t_i \approx 35^\circ\text{C}$  for  $c = 1\text{ M}$ ,  $t_i \approx 40^\circ\text{C}$  for  $c = 0.1\text{ M}$ , and  $t_i > 45^\circ\text{C}$  for  $c = 0.01\text{ M}$ ).

(iii) *The effect of solvent dielectric constant ( $\epsilon$ ):*

At a given temperature,  $z_p$  decreases when  $\epsilon$  decreases. Furthermore, there is no charge–discharge transition when heavy water ( $\text{D}_2\text{O}$ ) is used as solvent.

(iv) *The effect of conformation:*

Macromolecules with a compact sphere conformation do exhibit a charge–discharge transition, but macromolecules with a non-free unwinding coil conformation do not. No conformational changes which could affect the diffusion coefficient were observed under the experimental conditions responsible for the transition (except when an external electric field was applied).

(v) *The effect of counterion:*

The charge–discharge transition is observed for different electrolytes. No particular counterion appears to be responsible for this phenomenon.

(vi) *The effect of aggregation:*

Surface tension measurements at different temperatures and gel chromatography gave strong evidence against aggregation [4]. Therefore, the possibility of polyelectrolyte aggregation as an explanation for the loss of charge must be ruled out.

Before giving the theoretical model, we present a brief, intuitive reasoning which could explain the charge–discharge transition. Later, we derive the basic equations of the model, and compare them with the experimental observations. Finally, the achievements, weaknesses and limitations of the theory are discussed.

Many macromolecules of biological importance (e.g. proteins) behave as charged polyelectrolytes when in aqueous solution [8], and their effective charge numbers determine their physicochemical properties. In this sense, the physical model considered here can also be of utility for spherical macromolecules other than lignosulfonate.

## 2. Intuitive explanation of the charge–discharge transition

Let us introduce the following plausible assumption in order to explain the effect of temperature on the effective charge number. At a certain temperature, a significant part of the coordination water surrounding the polyelectrolyte charged groups (sulfonate groups in this case) is lost. This coordination water can be assumed to be distributed in one or two hydration shells around the charged groups. The shells prevent the contribution of the low dielectric medium formed by the polyelectrolyte body. The thermal energy  $kT$  is smaller than the electrostatic energy  $e_1$  associated with the water molecules adjacent to the charged groups of the polyelectrolyte (first hydration shell)

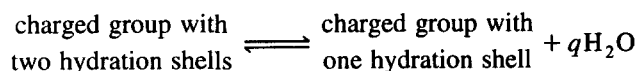
$$e_1 = p_w E_1 \approx p_w \frac{e}{4\pi\epsilon_0\epsilon_1 r_1^2} \sim 10^{-20}\text{ J} > kT \quad (1)$$

but greater than the electrostatic energy  $e_{II}$  associated with the water molecules in the second hydration shell

$$e_{II} = p_w E_{II} \approx p_w \frac{e}{4\pi\epsilon_0\epsilon_{II} r_{II}^2} \sim 10^{-21}\text{ J} \lesssim kT \quad (2)$$

where  $r_I \approx 4 \text{ \AA}$  and  $r_{II} \approx 7 \text{ \AA}$  (see Fig. 1). The estimations in Eqs. (1) and (2) assume that the main contribution to the energies  $e_I$  and  $e_{II}$  results from the electrostatic interaction between the water molecules and the charged group. Here  $E_I$  and  $E_{II}$  denote the electric fields created by the charged group in the first and second hydration shells, respectively,  $p_w$  is the electric dipole moment of the water molecule,  $k$  is the Boltzmann constant,  $T$  is the absolute temperature, and  $e$  is the elementary electric charge. The values  $\epsilon_I \approx 6$  and  $\epsilon_{II} \approx 40$  used in the previous estimations are typical values for the first and second water layers at the surface of charged interfaces respectively.

Consequently, thermal energy can destroy the second hydration shell but not the first hydration shell. When this destruction occurs, the counterion sees a low dielectric medium (since  $\epsilon_I \ll \epsilon_{II}$ ) and then association takes place. The fact that the charge–discharge transition is observed in a relatively small temperature range  $\Delta T$  centered at a given temperature  $T_i$  could be due to the existence of some cooperative effect [9] in the transition:



where  $q$  is the number of water molecules in the second hydration shell.

It should be mentioned in this context that two kinds of water molecules associated with proteins have been identified when studying protein–water interactions by dielectric methods [10]: internal water (a strongly bound hydration layer which extends no more than one to two water molecule diameters beyond the protein surface), and peripheral, not so tightly bound, water. A critical hydration level [10] appears to be required to establish, for example enzymatic activity. Here, a second hydration shell is proposed to be critical for the polyelectrolyte to keep its charge. Note also that the existence or not of this charge

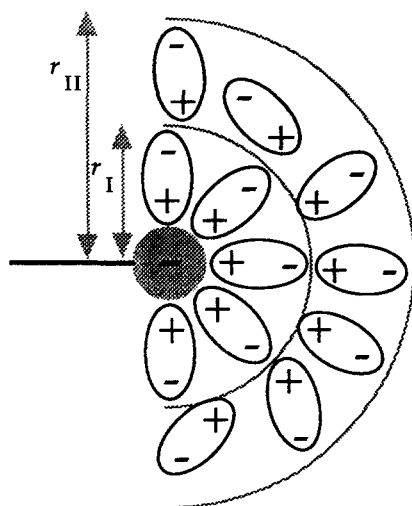


Fig. 1. Schematic view of a polyelectrolyte charged group and the water molecules around it (hydration shells I and II).

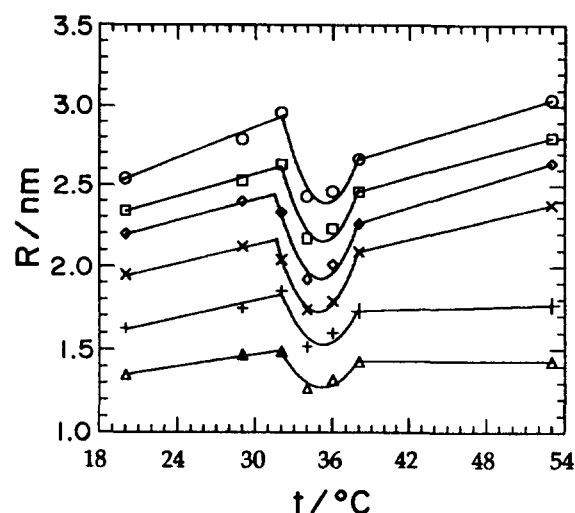


Fig. 2. Polyelectrolyte radius vs. temperature. The radii were estimated from the Stokes–Einstein equation and the diffusion coefficients of lignosulfonate in 0.1 M NaCl aqueous solution. The experimental points correspond to the molar masses 50000 ( $\circ$ ), 40000 ( $\square$ ), 30000 ( $\diamond$ ), 20000 ( $\times$ ), 10000 ( $+$ ), and 5000 ( $\triangle$ )  $\text{g mol}^{-1}$ .

will determine the behavior of the polyelectrolyte in solution.

The loss of the second hydration shell is not just a reasonable assumption to explain the transition observed experimentally. It becomes an experimental fact if we estimate the polyelectrolyte radius  $R$  from the diffusion coefficient  $D$  measured at several temperatures by means of the Stokes–Einstein equation:

$$R = \frac{kT}{6\pi\eta D} \quad (3)$$

where  $\eta(T)$  is the solution viscosity, assumed to be that of pure water since the solution is very dilute with respect to polyelectrolyte. Fig. 2 shows the effective polyelectrolyte radius as estimated from Eq. (3). The new measurements were carried out following the procedure stated in Ref. [1]. Four regions can be distinguished in this plot.

(1) *Before the transition region* ( $t < 32^\circ\text{C}$ ). Point(i) in the previous section stated that ion binding increases with temperature in this region. This binding between a hydrated counterion and a charged group with two hydration shells takes place with sharing of the second hydration shell (see states ① and ② in Fig. 3), and therefore it produces an increase of 3–4  $\text{\AA}$  in the radius of the group. However, since only a small number of groups become associated, the effective radius of the polyelectrolyte only increases by 1 or 2  $\text{\AA}$  (see Fig. 2).

(2) *Just before the transition temperature* ( $32^\circ\text{C} < t < 35^\circ\text{C}$ ). The radius of the polyelectrolyte decreases sharply by about 3  $\text{\AA}$  (i.e. one water molecule diameter, see Fig. 2). This suggests the loss of the second hydration layer in

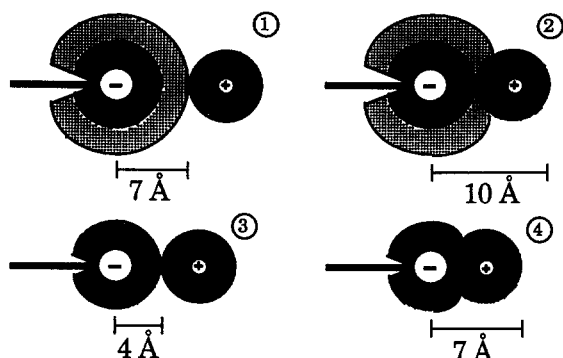


Fig. 3. The proposed scheme for hydration-mediated ion binding to the charged groups of lignosulfonate. Two possible hydration states are considered for the charged groups: state ① with two hydration shells, and state ③ with only the primary hydration shell. The criterion for ion binding is the sharing of the (primary) hydration shell of the counterion with the outer hydration shell of the charged group (states ② and ④). The distances shown in the figure indicate roughly the size of the charged and uncharged groups.

most of the charged groups (see states ① and ③ in Fig. 3).

(3) *Just after the transition temperature* ( $35^{\circ}\text{C} < t < 38^{\circ}\text{C}$ ). The radius of the polyelectrolyte increases sharply by about 2–3 Å (see Fig. 2). This suggests that the binding of the hydrated counterion with the (singly hydrated) charged group takes place with sharing of the first hydration layer. In principle, this binding should imply an increase in radius of some 3–4 Å (see states ③ and ④ in Fig. 3). However, it must be noted that the (dramatic) loss of the surface charge implies some shrinking of the macromolecule as a consequence of the elastic forces. This shrinking should be more noticeable for the larger macromolecules. Fig. 2 shows indeed that the difference in the radii corresponding to  $32^{\circ}\text{C}$  and  $38^{\circ}\text{C}$  increases significantly with the molar mass of the macromolecule.

(4) *After the transition region* ( $t > 38^{\circ}\text{C}$ ). The radius of the polyelectrolyte increases smoothly, which could be attributed to a thermal expansion of the polyelectrolyte as well as to the fact that the solution viscosity could deviate from that of pure water at these temperatures.

The interpretation of the results in Fig. 2 on the basis of the crude model in Fig. 3 could give additional credit to the assumption of the loss of the second hydration shell as being the responsible for ion binding. However, we should recognize the speculative nature of the above ideas, which were motivated by the absence of direct evidence about the structure of the polyelectrolyte charged groups. In particular, detailed information on the water molecule–charged group interaction is lacking.

It has been confirmed experimentally from dielectric studies of proteins [10] that the extent of association of the bound water is such that it can be considered as a shell that contributes to the protein effective radius of rotation when

an external electric field is applied. Therefore, the water shells should also affect the effective transport radius given by Eq. (3). (Note that the hydrated charged groups are located at the external polyelectrolyte surface.)

### 3. Theoretical model

The theoretical model considered here ignores the electrostatic interaction between neighboring charged groups at the polyelectrolyte surface. The basis for proceeding in this way can be found in Appendix A, where the problem of distributing  $N$  point charges homogeneously on the surface of a sphere of radius  $R$  is analyzed. It is concluded there that the distance  $d$  between the charged groups is of the order of the polyelectrolyte radius ( $d \approx R \approx 15$  to  $35$  Å) since most of the experimental situations dealt with here have  $N \approx 10$  (see Table 1A in Appendix A). This means that the charged groups at the protein surface can be effectively screened by the surrounding electrolyte aqueous solution except for very low electrolyte concentrations (see Ref. [11] in this context). Moreover, it seems clear from the preceding section that the charge–discharge transition is related to changes in the hydration shells of the charged groups with temperature rather than to some particular electrostatic interaction between these groups. In this context, the experimental fact that the surface charge density is independent of the polyelectrolyte molar mass [1] could also give support to the assumption of ignoring the electrostatic interaction between the polyelectrolyte charged groups for the whole range of molar masses studied [1,4]. Let us mention finally that if the (repulsive) electrostatic interaction between the charged groups at the polyelectrolyte surface were important, an increase in the electrolyte concentration would act to suppress this interaction, and then higher temperatures would be required for the charged polyelectrolyte to become unstable [12]. This trend is just the opposite to that observed experimentally [1,4].

According to the above ideas, any attempt to explain the temperature behavior of the polyelectrolyte must account for the changes in the hydration shells of the charged groups. Also, it must incorporate the fact that the polyelectrolyte is a compact sphere [1] under our experimental conditions. The above questions make difficult the application of the classical concepts of the Debye–Hückel theory [13] as well as the existing models for ion binding to homogeneously charged chains and rod-like polyelectrolytes [14] to our problem. It would be possible, however, to employ the classical theories of ion association in electrolyte solutions [7], and describe the changes in the hydration shells by means of a particular temperature dependence of the dielectric constant  $\epsilon$  of the medium where association occurs. This procedure has been followed in complex solvents where ion binding is strongly affected by, for example, a polymer matrix environment

(see Ref. [15] and references cited therein for a critical examination of the procedure as well as for alternative theories). If we describe the ion association between two ions of charge numbers  $z_1 = 1 = -z_2$  by means of an association constant of the form [7,16]

$$K_a \approx \exp(e^2/4\pi\epsilon_0\epsilon akT) \quad (4a)$$

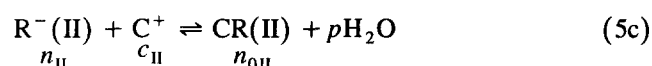
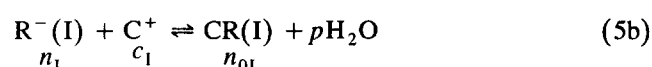
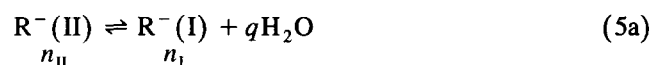
where  $a$  is the distance of closest approach between ions, then

$$\frac{d \ln K_a}{dT} = - \frac{e^2}{4\pi\epsilon_0 ak(\epsilon T)^2} \frac{d(\epsilon T)}{dT} \quad (4b)$$

Eq. (4b) allows for describing the observed changes in the association constant  $K_a$  with temperature through the temperature dependence of the dielectric constant  $\epsilon(T)$ . In particular, this equation predicts an increase of association with temperature if the product  $\epsilon T$  decreases with  $T$ , which is the case for many liquids at room temperature.

Although it is in principle possible to describe the changes in the hydration shells (and then the experimental results) from a particular adjustable curve  $\epsilon(T)$ , we have followed here a different more definite approach based on the relative populations of the different hydration states assumed for the charged groups. This approach is consistent with the experimental results presented in Fig. 2, and incorporates the basic ideas of the so-called “ $n$ -states” models employed in the study of biopolymers and membrane ionomers [17].

Let us consider the following scheme for the ion association reactions:



In Eqs. (5a)–(5c),  $C^+$ ,  $R^-(I)$ ,  $R^-(II)$ ,  $CR(I)$ , and  $CR(II)$  denote the counterion (sodium ion), the charged (sulfonate) group with one hydration shell, the charged group with two hydration shells, the ion pair (sodium sulfonate) with one layer of water in between, and the ion pair with two layers of water in between respectively. Also,  $c_I$ ,  $c_{II}$ ,  $n_I$ ,  $n_{II}$ ,  $n_{OI}$ , and  $n_{OII}$  denote the concentrations of  $C^+$  in the vicinity of  $R^-(I)$ ,  $C^+$  in the vicinity of  $R^-(II)$ ,  $R^-(I)$ ,  $R^-(II)$ ,  $CR(I)$  and  $CR(II)$  respectively. Ion binding in steps (5b) and (5c) takes place with sharing of the hydration shells and unbinding of a number  $p$  of water molecules. Fig. 3 can be considered as a crude, schematic representation of the previous steps. In particular, step (5a) implies the change from state ① to state ③ in Fig. 3; step (5b) implies the change from state ③ to ④; and finally step (5c) implies the change from state ① to ②.

According to the assumptions introduced in Section 2, the forward rate constant of step (5a) is much greater than

the backward rate constant at high enough temperatures ( $T \geq T_i$ ), and thus almost all of the  $R^-(II)$  groups become  $R^-(I)$  groups in a narrow temperature range  $\Delta T \ll T_i$  centered at  $T_i$ . However, step (5b) is so fast (see below) that the concentration of the  $R^-(I)$  groups remains much smaller than the concentration of  $R^-(II)$  groups at all temperatures. Therefore, we could say that almost all of the  $R^-(I)$  become  $CR(I)$  in a very small temperature range.

At  $T < T_i$  virtually no  $R^-(I)$  group is formed (see Fig. 2) and ion binding takes place through step (5c). The resulting association constant is then very small, because the counterions “see” the charged groups separated by two hydration layers, and then most of the  $R^-(II)$  groups remain dissociated. At  $T \geq T_i$  the situation is very different, however. In this case, the counterions can “see” almost immediately any  $R^-(I)$  group recently formed, and thus ion binding increases considerably (step 5b). (Note that this group is attached to the low dielectric medium formed by the polyelectrolyte body, and separated by only one hydration shell from the counterion.) The scheme formed by steps (5a)–(5c) can thus provide a reasonable explanation for the temperature dependence of the charge number of the polyelectrolyte in a wide temperature range.

Let us put the above ideas on a quantitative basis. First, we consider steps (5a) and (5b), which are responsible for the charge–discharge transition. (Later on, step (5c) will be employed to account for the ion binding at lower temperatures,  $T < T_i$ .) Let  $\epsilon_1$  be the total energy needed to remove the second hydration shell from a charged group. From Eq. (5a) we can write

$$n_I/n_{II} = \exp(-\epsilon_1/kT) \quad (6a)$$

where  $\epsilon_1 \approx q\epsilon_{II} \leq qkT_i$  according to the assumptions introduced in Section 2. Step (5b) leads to

$$n_{OI}/n_I = A \exp(-\epsilon_2/kT) \quad (6b)$$

where the constant  $A$  should be proportional to the counterion concentration  $c_I$  (and then to the bulk electrolyte concentration  $c$ ), and  $\epsilon_2 \gg kT_i$  is the (electrostatic plus hydration) energy associated with the ion pair formation given by step (5b). From Eqs. (6a) and (6b),

$$\begin{aligned} \frac{1-\theta}{\theta} &= \frac{n_{OI} + n_{OII}}{n_I + n_{II}} \approx \frac{n_{OI}}{n_I + n_{II}} = A \frac{\exp(-\epsilon_2/kT)}{1 + \exp(\epsilon_1/kT)} \\ &\approx A \exp[-(\epsilon_1 + \epsilon_2)/kT] \end{aligned} \quad (7)$$

where  $\theta \equiv (n_I + n_{II})/(n_{OI} + n_{OII} + n_I + n_{II})$  is the fraction of charged groups at the polyelectrolyte surface. Note that both  $\epsilon_1$  and  $\epsilon_2$  are positive. By defining the transition temperature  $T_i$  from the condition  $\theta(T = T_i) = 0.5$ , Eq. (7) can be rewritten in the form

$$\frac{1-\theta}{\theta} = \exp\left\{\frac{\epsilon_1 + \epsilon_2}{k} \left(\frac{1}{T_i} - \frac{1}{T}\right)\right\} \quad (8)$$

Finally, the absolute value of the effective (as obtained

from transport measurements [1,4]) polyelectrolyte charge number can be expressed as

$$z_p = \theta z_m = z_m / \left[ 1 + \exp \left\{ \frac{\epsilon_1 + \epsilon_2}{kT_i} \frac{T - T_i}{T} \right\} \right] \quad (9)$$

where  $z_m$  is the absolute value of the polyelectrolyte charge number at a reference temperature lower than  $T_i$ . Note that  $z_m$  increases with the molar mass  $M$  of the polyelectrolyte [1]. Eq. (9) is formally similar to that characteristic of the folded–unfolded transition in proteins [18], and can now be compared with the experimental  $z_p$  vs.  $T$  curve for each polyelectrolyte fraction, i.e. for each value of the average molar mass  $M$ . It should be stressed that the theory predicts that both  $T_i$  and  $(\epsilon_1 + \epsilon_2)$  should be independent of  $M$ . Indeed, the theory deals with isolated charged groups at the polyelectrolyte surface, and these must have similar values of  $(\epsilon_1 + \epsilon_2)$  and  $T_i$  regardless of the molar mass  $M$  of the polyelectrolyte. Fig. 4 shows that this is indeed the case. Eq. (9) gives a quantitative agreement between theory (continuous lines) and experiment (points) when  $T_i = 307.6$  K and  $(\epsilon_1 + \epsilon_2)/kT_i = 257$ . The free energy of hydration [16,19] of sodium ion at 25°C is  $375 \text{ kJ mol}^{-1} \approx 145kT_i$ , and though the latter value could be modified in our case because of the low dielectric constant of the polyelectrolyte and the corresponding image charge effects [20], the result obtained for  $\epsilon_1 + \epsilon_2$  is still very large. In particular, the energy  $\epsilon_2$  describing the counterion binding is of the order of those characteristic of a covalent bond (see Nagasawa [13], covalent bonds have energies in the range 100–1000 kJ), which means that the binding is very strong. Also, the energy  $\epsilon_1$  could be greater than estimated because of the

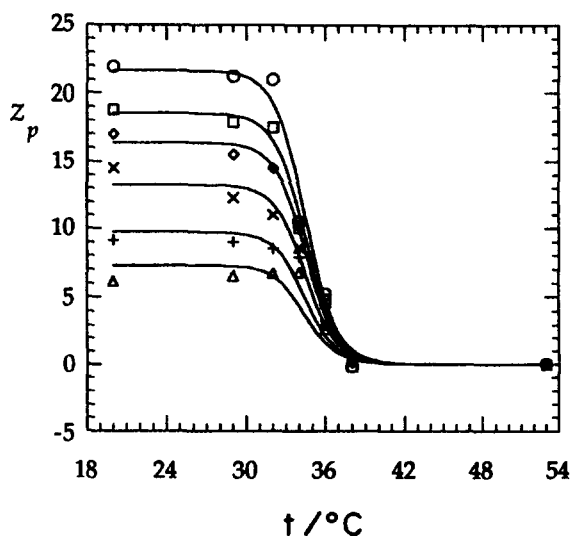


Fig. 4. Effective charge number (absolute value) vs. temperature corresponding to lignosulfonate in 0.1 M NaCl aqueous solution. The experimental points are those included in Fig. 2. The theoretical (continuous) lines correspond to Eq. (9) in the text.

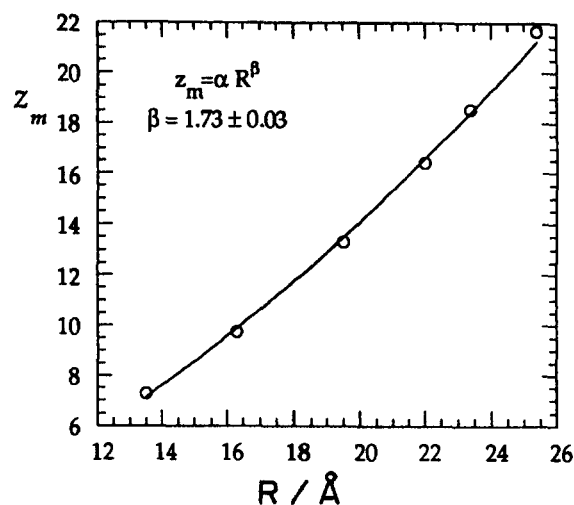


Fig. 5.  $z_m$  vs. polyelectrolyte radius at 20°C. The  $z_m$  values were obtained from Fig. 4 and Eq. (9) for the different radii (molar masses) in Fig. 2. Note that  $z_m/R^2$  is approximately constant with the molar mass of the polyelectrolyte fraction.

interaction between the hydration water molecules and the polyelectrolyte. Indeed, in spite of the large differences in hydration energy, the characteristics of the charge–discharge transition were essentially the same for several monovalent counterions [4], and this supports the idea that  $\epsilon_1$  is markedly influenced by the interaction between the hydration water molecules and the polyelectrolyte. Finally, we must mention the entropy effects associated with the loss of the second water shell. Every water molecule leaving this shell and being incorporated to the bulk solvent has additional translational degrees. However, the entropic contribution to the free energy change of the charge–discharge transition has not been explicitly accounted for, and should therefore be included in the value of the adjustable parameter  $(\epsilon_1 + \epsilon_2)$ . When an ion pair is formed, there is an important rearrangement of solvent molecules around the new electrical structure created, and this should impact on both energy and entropy changes. Unfortunately, the lack of information on the structural properties of the ion pair makes it difficult to evaluate explicitly the above changes.

The results in Fig. 4 show an increase in the proportion of polyelectrolyte neutral groups when the number of water molecules at the charged groups diminishes, which agrees with the experimental findings in membrane ionomers [17]. Fig. 5 shows the charge number  $z_m$  as a function of the polyelectrolyte radius at 20°C [4]. The surface charge density is approximately constant with the molar mass of the polyelectrolyte, which agrees with previous observations (see e.g. Table 3 of Ref. [1]).

Note finally that step (5c) has been ignored in the above treatment because the association constant corresponding to step (5b) is much greater than that corresponding to step

(5c). Also, we see from Eq. (6a) that most of the charged groups are in the  $R^-(II)$  form at all temperatures. However, when one of these becomes an  $R^-(I)$  group (owing to a thermal fluctuation, for instance), ion association occurs almost immediately because of the large value of energy  $\epsilon_2$ .

#### 4. Discussion

The theory presented here, though admittedly crude and speculative, can explain a number of experimental results for the temperature behavior of liginosulfonate. In particular, the temperature dependence of the effective charge number, including the charge–discharge transition, has been satisfactorily accounted for from a reduced number of assumptions. The classical theories describing ion association in electrolyte solutions [7] consider the solvent as a dielectric continuum, and cannot thus explain this sharp transition. There is some experimental evidence [3] that the theory could also be of utility for other spherical macromolecules.

Some limitations of the theory and important questions not dealt with in detail here are the following.

(i) *Cooperativity.* Since the charge–discharge transition occurs in a temperature range of a few degrees, a cooperative effect [9] between the water molecules at the charged groups could be responsible for the loss of the second hydration shell. The sharp increase in the forward rate of step (5a) at a given  $T_i$  (i.e. the rapid destruction of the second hydration shell) closely parallels the all or none behavior characteristic of cooperative transitions [9]. However, this cooperativity has not been explicitly introduced in the model. Again, the lack of detailed information on the water molecule–charged group interaction in complex systems (polyelectrolytes, charged membranes, etc.) [15,17,19,21] makes it difficult to propose a particular cooperative mechanism. Finally, although we have considered the loss of the second water shell, it should be noted that a change in the dielectric properties of the water shells [10] (not involving necessarily the loss of the second water shell), might also explain the increase in ion binding. However, the observed change in the diffusion coefficient of the polyelectrolyte (see Fig. 2) would then remain unexplained.

(ii) *Concentration effects.* The effects of concentration on the ion association are accounted for in the model through the relationship between  $T_i$ ,  $(\epsilon_1 + \epsilon_2)$  and  $A$  (a constant proportional to electrolyte concentration  $c$ , see Eqs. (5b) and (6b)), namely

$$A = \exp[(\epsilon_1 + \epsilon_2)/kT_i] \quad (10)$$

Therefore, the electrolyte solution concentration  $c$  does not enter explicitly in Eq. (9). If we assume that  $(\epsilon_1 + \epsilon_2)$

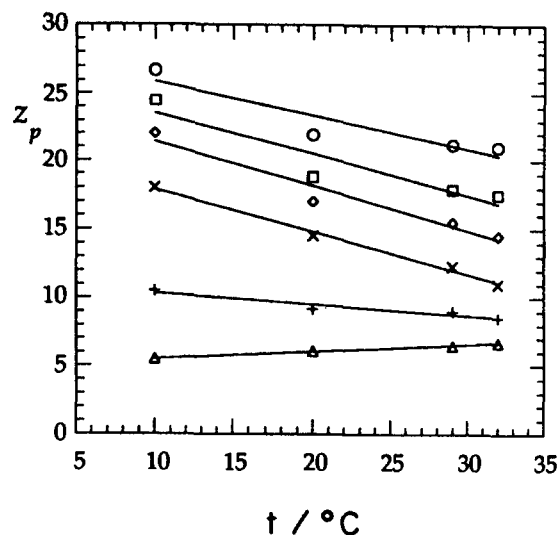


Fig. 6. Effective charge number (absolute value) vs. temperature for  $T < T_i$  under the same experimental conditions as for Fig. 4. The molar masses are those of Figs. 2 and 4. The theoretical (continuous) lines correspond to Eq. (13) in the text.

should not change very much with  $c$ , then the only parameter in Eq. (9) which depends on concentration is the temperature  $T_i$  (see point (ii) in Section 1). In the classical theories for ion association, the concentration  $c$  appears as a factor multiplying the exponential factor in the denominator. If we particularize Eq. (10) for two concentrations  $c$  and  $c'$ , we can readily obtain the relationship

$$\ln \frac{c'}{c} = \frac{\epsilon_1 + \epsilon_2}{k} \left( \frac{1}{T_i(c')} - \frac{1}{T_i(c)} \right) \quad (11)$$

which predicts the transition temperature  $T_i(c')$  from a known value  $T_i(c)$ . We have from Fig. 4 that  $T_i(0.1 \text{ M}) \approx 307.6 \text{ K}$ , and then Eq. (11) gives  $T_i(1 \text{ M}) \approx 304.7 \text{ K}$  and  $T_i(0.01 \text{ M}) \approx 310.2 \text{ K}$ . These values follow the experimental trends [4], though the latter temperature seems to be lower than the observed value. Note however that  $T_i$  corresponds to  $\theta = 0.5$ , and not to  $\theta \approx 0$ . Bearing in mind this fact, the agreement between Eq. (11) and the experimental values in Table 5 of Ref. [4] is reasonable.

(iii) *Polyelectrolyte behavior at  $T < T_i$ .* The mechanism (5a)–(5b) is not important in this temperature range, and ion binding should follow step (5c) (or a similar mechanism). Yet, the classical Bjerrum and Fuoss theories [7] do not apply either, since Fig. 6 shows that  $K_a$  increases with temperature for the polyelectrolyte fractions of higher molar masses while it decreases with temperature for the fractions of lower molar masses. This “size effect” could suggest that the counterion “sees” the polyelectrolyte body (and not only a particular charged group). Indeed, if we describe step (5c) quantitatively by

$$n_{0II}/n_{II} = B \exp(-\epsilon_3/kT) \quad (12)$$

and

$$\theta = \frac{n_I + n_{II}}{n_{OI} + n_{OII} + n_I + n_{II}} \approx \frac{n_{II}}{n_{OII} + n_{II}}$$

$$= \frac{1}{1 + B \exp(-\epsilon_3/kT)} \quad (13)$$

where  $B$  is a constant proportional to  $c_{II}$  (and then to  $c$ ), the following values are obtained for the electrostatic plus hydration energy  $\epsilon_3$ :  $3.0kT_i$  ( $M = 50\,000$ ),  $4.2kT_i$  ( $M = 40\,000$ ),  $4.8kT_i$  ( $M = 30\,000$ ),  $5.6kT_i$  ( $M = 20\,000$ ),  $2.0kT_i$  ( $M = 10\,000$ ), and  $-2.4kT_i$  ( $M = 5000$ ). As expected, these values are of a few  $kT_i$  units. The increase in ion binding with temperature observed for the larger polyelectrolyte fractions could be attributed to the fact that the ratio (water bound to the surface)/(volume of the low dielectric body of the polyelectrolyte) decreases with the size of the polyelectrolyte [10], which should enhance ion binding.

Note finally that the different signs of energy  $\epsilon_3$  can arise from the dominant term (hydration or electrostatic) in this energy. In this context, a local maximum has been obtained for the counterion concentration near a charged pore wall [22] just before the zone where hydration effects dominate over the electrostatic effects. (To bring two small ions of different sign into contact, one must remove the accompanying layers of solvent, and this process may require a considerable amount of energy, see e.g. Fig. 11 in Ref. [23].) Close enough to the charged pore wall, however, electrostatic attraction prevails again, and larger counterion concentrations are obtained [22]. Hydration forces can also dominate over coulombic and Van der Waals forces for small enough distances in the case of macroions in solution [24]. Therefore, the above values of  $\epsilon_3$  could be related to the different hydration and electrostatic energies characteristic of each polyelectrolyte fraction. This result emphasizes again the different nature of step (5c) when compared with steps (5a) and (5b), and can be clearly seen when comparing Figs. 4 and 6; the same value of  $(\epsilon_1 + \epsilon_2)$  applies to all molar masses in Fig. 4.

(iv) *Compact sphere vs. non-free unwinding coil.* It has been shown experimentally [4], using the Mark-Houwink equation, that the charge-discharge transition occurs only when the macromolecule is a compact sphere. It seems quite plausible that the penetration of the solvent inside the polyelectrolyte body should be much easier in a non-free unwinding coil than in a compact sphere. Furthermore, some solvent can be trapped into clusters in the coil, and step (5a) would perhaps need much higher temperatures to occur in this case.

For the case of a compact sphere in solvents other than pure water [5], steps (5a) and (5b) could still apply, but now the energies  $\epsilon_1$  and  $\epsilon_2$  involved must change according to the solvent dielectric constant. In particular, a decrease in the dielectric constant should promote ion binding because of the corresponding increase in energy

$\epsilon_2$ . Also, step (5a) could be inhibited in a highly structured solvent ( $D_2O$ , for example), which should impact in turn on the energy  $\epsilon_1$ . Therefore, other experimental results [2,4,5] could also be rationalized from the basic ideas included in the model.

## Acknowledgement

The authors thank Professor Julio Pellicer for his continuous assistance and advice.

## References

- [1] A.K. Kontturi, J. Chem. Soc., Faraday Trans. I, 84 (1988) 4033, 4043.
- [2] A.K. Kontturi, K. Kontturi and P. Niinikoski, J. Chem. Soc., Faraday Trans., 87 (1991) 1779.
- [3] A.K. Kontturi, K. Kontturi, P. Niinikoski, A. Savonen and M. Vuoristo, Acta Chem. Scand., 46 (1992) 348.
- [4] A.K. Kontturi, K. Kontturi, P. Niinikoski and L. Murtomäki, Acta Chem. Scand., 46 (1992) 941.
- [5] A.K. Kontturi and K. Parovuori, Acta Chem. Scand., 47 (1993) 529.
- [6] A.K. Kontturi, K. Kontturi and P. Niinikoski, J. Chem. Soc., Faraday Trans., 86 (1990) 3097.
- [7] A.K. Kontturi and K. Kontturi, J. Colloid Interface Sci., 120 (1987) 256; 124 (1988) 328.
- [8] J.O'M. Bockris and A.K.N. Reddy, Modern Electrochemistry, Plenum, New York, 1976, Chapter 3. Y. Marcus, Ion Solvation, Wiley, New York, 1985, Chapter 8.
- [9] S. Ohki, in S. Srinivasan, Y.A. Chizmadzhev, J.O'M. Bockris, B.E. Conway and E. Yeager (eds.), Bioelectrochemistry, Vol. 10, Comprehensive Treatise of Electrochemistry, Plenum, New York, 1985, pp. 1–130.
- [10] A. Warshel and S.T. Russell, Q. Rev. Biophys., 17 (1984) 283.
- [11] J. Engel, in W. Hoppe, W. Lohmann, H. Markl and H. Ziegler (eds.), Biophysics, Springer, Berlin, 1983, pp. 233–243.
- [12] R. Pethig, Annu. Rev. Phys. Chem., 43 (1992) 177.
- [13] S. Mafé, J.A. Manzanares and H. Reiss, J. Chem. Phys., 98 (1993) 2325.
- [14] J. Koryta, Ions, Electrodes and Membranes, Wiley, New York, 1991, Chapter 1.
- [15] S.N. Timashev, in S.N. Timashev and G.D. Fasman (eds.), Biological Polyelectrolytes, Vol. 3, Biological Macromolecules, Marcel Dekker, New York, 1970, pp. 1–64.
- [16] M. Nagasawa, in E. Sèlègny (ed.), Polyelectrolytes, Reidel, Dordrecht, 1974, pp. 57–77.
- [17] B.E. Conway, Ionic Hydration in Chemistry and Biophysics, Elsevier, Amsterdam, 1981, Chapter 19 and 34.
- [18] H. Berg, in W. Hoppe, W. Lohmann, H. Markl and H. Ziegler (eds.), Biophysics, Springer, Berlin, 1983, pp. 258–264.
- [19] M.A. Cohen Stuart, G.J. Fleer, J. Lyklema, W. Norde and J.M.H.M. Scheutjens, Adv. Colloid Interface Sci., 34 (1991) 477.
- [20] S. Kawaguchi, T. Kitano, K. Ito and A. Minakata, Macromolecules, 23 (1990) 731.
- [21] T. Nishio, Biophys. Chem., 40 (1991) 19; 49 (1994) 201.
- [22] R. Olender and A. Nitzan, Electrochim. Acta, 37 (1992) 1505.
- [23] R. Olender and A. Nitzan, J. Chem. Phys., 100 (1994) 705.
- [24] R.A. Robinson and R.H. Stokes, Electrolyte Solutions, Butterworths, London, 1959, Chapter 3.
- [25] K.A. Mauritz and A.J. Hopfinger, in J.O'M. Bockris, B.E. Conway and R.E. White (eds.), Modern Aspects of Electrochemistry, Vol. 14, Plenum, New York, 1982, pp. 425–508.



- [18] A. Ben-Naim, *Statistical Thermodynamics for Chemists and Biochemists*, Plenum, New York, 1992; Chapter 4.
- [19] A. Warshel and J. Åquist, *Annu. Rev. Biophys. Chem.*, 20 (1991) 267.
- [20] J.O'M. Bockris and A.K.N. Reddy, *Modern Electrochemistry*, Plenum, New York, 1976, Chapter 7.
- [21] K.J. Irwin, S.M. Barnett and D.L. Freeman, *J. Membr. Sci.*, 47 (1989) 79.  
M. Schlenkrich, K. Nicklas, J. Brickmann and B. Bopp, *Ber. Bunsenges. Phys. Chem.*, 94 (1990) 133.
- [22] M.W. Verbrugge, E.W. Schneider, R.S. Conell and R.F. Hill, *J. Electrochem. Soc.*, 139 (1992) 3421.  
A.G. Guzmán-García, P.N. Pintauro, M.W. Verbrugge and R.F. Hill, *AIChE J.*, 36 (1990) 1061.
- [23] T.E. Hogen-Esch and J. Smid, *J. Am. Chem. Soc.*, 88 (1966) 307.
- [24] K.S. Schmitz, *Macroions in Solution and Colloidal Suspension*, VCH, New York, 1993, p. 114.
- [25] M. Abramowitz and I.A. Stegun, *Handbook of Mathematical Functions*, Dover, New York, 1972, p. 79.

### Appendix A: homogeneous distribution of $N$ point charges on a spherical surface of radius $R$

In general, a given number  $N$  of point charges cannot always be distributed homogeneously on a spherical surface. The homogenous distribution is only possible for  $N = 2, 3, 4, 6$ , and 12. For all the other cases, the distance between charges will differ slightly from one pair to another. However, we can estimate the average distance between charges by assuming that they are homogeneously distributed. In this case, three neighboring point charges would define a regular spherical triangle of inner angle  $A$  and side angle  $a$  (see Fig. 1A). The number of such triangles could be obtained either from the number of point charges per triangle

No. of spherical triangles

$$= \frac{\text{Total no. of point charges}}{\text{No. of point charges per triangle}} = \frac{N}{3A/2\pi} \quad (\text{A1})$$

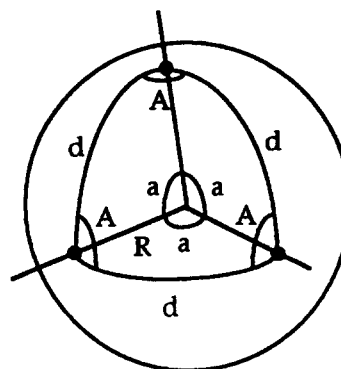


Fig. A1. Three neighboring point charges defining a regular spherical triangle of inner angle  $A$  and side angle  $a$  on the surface of a sphere of radius  $R$ .

or from the area of the triangle [25]

No. of spherical triangles

$$= \frac{\text{Total area}}{\text{Area of the triangle}} = \frac{4\pi R^2}{(3A - \pi)R^2} \quad (\text{A2})$$

Therefore, the inner angle can be related to  $N$  through

$$A = \frac{\pi}{3} \frac{N}{N-2} \quad (\text{A3})$$

The distance between neighboring charges is given (see Fig. 1A) by

$$d = aR = \arccos\left(\frac{\cos A}{1 - \cos A}\right)R \quad (\text{A4})$$

where the cosine theorem of spherical trigonometry [25] has been used to relate  $a$  and  $A$ . Table 1A shows some values of the ratio  $d/R$  as a function of the number of charges  $N$ . From this table, it can be concluded that  $d \approx R$  for  $N \approx 10$ .

Table A1  
 $d/R$  as a function of the number of changes  $N$

$N$	4	6	8	10	15	20	30	40
$d/R$	1.91	1.57	1.36	1.21	0.99	0.86	0.70	0.60